2015-04-06

The Surfactant Dipalmitoylphophatidylcholine (DPPC) Modifies Acute Responses in Alveolar Carcinoma Cells in Response to Low Dose Silver Nanoparticle Exposure

Gordon Chambers
Technological University Dublin, Gordon.chambers@tudublin.ie

Anna Murphy
Technological University Dublin, anna.murphy3@tudublin.ie

Kate Sheehy
Technological University Dublin

See next page for additional authors

Recommended Citation

Chambers, G., Murphy, A., Sheehy, K. & Casey, A. (2015). The surfactant dipalmitoylphophatidylcholine modifies acute responses in alveolar carcinoma cells in response to low-dose silver nanoparticle exposure. *Journal of Applied Toxicology* 35, pp.1141–1149. doi: 10.1002/jat.3148

Funder: SCIENCE FUNDATION IRELAND

The surfactant dipalmitoylphophatidylcholine (DPPC) Modifies Acute Responses in Alveolar Carcinoma cells in response to low dose Silver Nanoparticle Exposure

A. Murphy*[1], K. Sheehy[1], A. Casey[1], G. Chambers[1, 2]

1. *Nanolab Research Centre, Focas Institute, Dublin Institute of Technology, Kevin Street, Dublin 8, Ireland*
2. *School of Physics, Dublin Institute of Technology, Kevin Street, Dublin 8, Ireland*

*Corresponding Author E-mail: anna.murphy3@mydit.ie Ph: +35314027932 Fax: +35314027901.

Abstract

Nanotechnology is a rapidly growing field with silver (AgNP) nanoparticles in particular utilized in a wide variety of consumer products. This has presented a number of concerns relating to exposure and the associated toxicity to humans and the environment. As inhalation is the most common exposure route, this study investigates the potential toxicity of AgNP to A549 alveolar epithelial carcinoma cells and the influence of a major component of lung surfactant dipalmitoylphosphatidylcholine (DPPC) on toxicity. It was illustrated that exposure to AgNP generated low levels of oxidative stress and a reduction in cell viability. While the presence of DPPC caused no influence on viability studies its presence increased reactive oxygen species (ROS) formation. DPPC also significantly modified the inflammatory response generated by AgNP exposure. These findings suggest a possible interaction between AgNP and DPPC causing particles to become more reactive thus increasing oxidative insult and inflammatory response within A549 cells.

Short Abstract

Inhalation presents as the most common route of silver (AgNP) nanoparticle exposure. As such its interaction with pulmonary surfactant may influence the biological response induced. Toxicological testing was performed on the A549 cell line and demonstrated toxicity induced by AgNP exposure. Significant changes in acute responses including ROS generation and inflammatory marker release was noted. It is postulated the presence of DPPC interacts with

AgNP producing a more reactive particle resulting in modification of acute responses at low dose exposures.

Introduction

Nanoparticle exposure via inhalation is probably the most common entry point for nanoparticles and during recent decades the generation of engineered nanoparticles for applications in medicine, food, cosmetics and electronics to name a few has increased the likelihood of exposure exponentially (Sozar & Kokini, 2009; Bouwmeester *et al*, 2009).

Inhalation provides an easy entry route for engineered nanoparticles in nano-carrier systems for drug delivery allowing an easy route for targeted, controlled and non-invasive delivery. Liposomes in particular have been the nano-carrier of choice in the development of improved and intelligent drug delivery systems (Varez-Lorenzo *et al*, 2009; Shum *et al*, 2001). While inhalation provides an alternative method of pharmaceutical delivery, improving both the treatment and comfort of patients, it can be a double edged sword and increase the delivery of undesirable effects of nanoparticles. A number of studies have been undertaken to explore lung entry of various nanoparticles and their subsequent distribution around the body. Cerium oxide (CeO_2) nanoparticles have been shown to cause acute toxicity in the lungs following exposure. It was postulated that this could possibly lead to chronic inflammation days after the exposure period with particles deposited in the lungs as they penetrate through the alveolar wall into the systemic circulation (Srinivas *et al*, 2010). Silver (AgNP) nanoparticle exposure in the lung has also been shown to induce cytotoxicity along with zinc oxide (ZnO) and titanium dioxide (TiO_2). Although all nanometals induced toxicity they did so at differing levels with ZnO inducing greater levels of toxicity in alveolar macrophages compared with the other two nanometals. The induced toxicity may also lead to excessive secretion of certain biological agents causing dysfunction in the cytokine network, reducing the efficiency of the respiratory immune system (Liu *et al*, 2013).

Due mainly to their antibacterial qualities AgNP are currently one of the most utilized nanomaterials on the market providing a diverse range of applications including medical devices, antibacterial textiles and toys and food packaging (Sozar & Kokini, 2009; Bouwmeester *et al*, 2009). While AgNP have been highly regarded for their benefits, their increased incorporation into everyday consumer products has generated considerable interest in establishing the risk exposure has on human health and the environment. A more in depth toxicological assessment of nanoparticle-biological interaction is required and a focus must now be shifted onto the influence of biofluids (any fluid within the body that can be secreted, excreted, obtained with a needle or develop due to a pathological process (Medicinenet)) and surfactants on toxicological outcome (Mwilu *et al*, 2013; Ehrenberg *et al*, 2009; Wang *et al*, 2013; Misra *et al*, 2012; Aggarwal *et al*, 2009). In light of this and the easy entry of nanoparticles both beneficial and otherwise, this study investigates the interaction and toxicological influence of a component of lung surfactant on AgNP toxicity on the lung.

Pulmonary surfactant is composed of a variety of complex phospholipids, lipids and surfactant specific proteins. Dipalmitoylphosphatidylcholine (DPPC) is the most abundant phospholipid, comprising 70-80% of total surfactant. The overall function is to reduce surface tension at the liquid-air interface at the bronchoalveolar surface (Kumar & Bohidar, 2010; Serrano & Perez-Gil, 2006). During inspiration, the surfactant lowers surface tension near equilibrium,

minimizing the work of breathing. During exhalation, surface tension values are reduced thus stabilizing the lungs at low air volume and preventing pulmonary oedema (Bakshi *et al*, 2008). In order to perform these functions all of the components of lung surfactant are required to work in conjunction. In recent studies DPPC has been used to improve the properties of liposomes to produce more successful *in vivo* methods of delivery. For example its inclusion in liposome encapsulation of cancer drugs can improve delivery of the complete drug concentration to tumour cells improving killing of cancer cells (Yavlovich *et al*, 2011).

The aim of this investigation is to assess the toxic response of a carcinogenic lung cell line, A549, to *in vitro* exposure to AgNP. The ability of DPPC to affect or modify any observed toxicity was also established. The physiochemical characteristics of nanoparticles play a vital role in toxicological investigation and as such analysis of AgNP was performed using dynamic light scattering analysis, UV-vis spectroscopy and zeta potential analysis. The effect of DPPC components on the size distribution and agglomerative state of AgNP was also investigated. A cytotoxic profile was carried out using a number of viability assays including 3-(4, 5-Dimethylthiazol-2-yl)-2, 5-diphenyltetrazolium bromide (MTT), alamar blue and a 2', 7'-dichlorofluorescin diacetate (DCFH-DA) plate assay to detect intracellular oxidative stress induced by exposure. The influence of DPPC on the outcome of toxicity was also assessed using the same assays and any interaction of DPPC with the physiochemical characteristics of AgNP determined. A subsequent study was performed to monitor the effect on the release of inflammatory markers interleukin-8 (IL-8) and tumour necrosis factor alpha (TNF-α) upon exposure to AgNP in the presence of DPPC.

Materials and Methods

Test materials and reagents

Polyvinylpyrrolidone (PVP) coated silver (Ag) nanopowder of < 100nm Catalogue No: 758329, was purchased from Sigma-Aldrich Ltd (Dublin-Ireland). PVP coating was confirmed by XRD analysis. 3-(4,5-Dimethylthiazol-2-yl)-2,5-diphenyltetrazolium bromide (MTT) Catalogue No: M5655 and 2',7'- dichlorofluorescin diacetate (DCFH-DA) Catalogue No: D6883 as well as cell culture media, supplements and trypsin were all purchased form Sigma-Aldrich Ltd (Ireland). Alamar blue (AB) was purchased from Biosciences (Dublin, Ireland). Dipalmitoylphosphatidylcholine (DPPC) was purchased from Sigma-Aldrich (Ireland).

Cell Culture

A549 (ATCC: CCL-185) an immortalized carcinogenic alveolar cell line was employed in this study. A549 cells were cultured in RPMI-1640 medium supplemented with 10% foetal bovine serum (FBS), 2mM L-glutamine and 45 IU/ml penicillin and 45 IU/ml streptomycin at 37°C in humidified 5% CO_2. All cell culture media including FBS other reagents and supplements were purchased from Sigma-Aldrich Ltd (Ireland).

Characterization of nanoparticles

Prior to the cytotoxicity testing, pristine AgNP were characterized as purchased and as prepared in various suspensions in the presence and absence of DPPC. The solutions of AgNP (15µg/ml) were prepared in deionised water (dH_2O) and RPMI-1640 cell culture media using a bath-sonicator for 20 minutes (Degussa-Ney ULTRAsonik 57X 50/60 Hz, California, USA) prior to size and zeta potential analysis. Dynamic light scattering and zeta potential measurements were performed with the aid of a Malvern ZetaSizer Nano ZS (Malvern Instruments, Worcestershire, UK) operating with version 5.10 of the systems Dispersion Technology Software (DTS Nano). For size measurement DTS0012 disposable sizing cuvettes were used. The samples were equilibrated at 25°C for 2 minutes before each measurement. For zeta potential analysis, DTS1060T clear disposable zeta cells were used and measurements were performed with the automatic model setting, using a voltage of five volts to minimize artefacts and charring of sample proteins during analysis.

Scanning Electron Microscopy (SEM) was also employed to estimate nanoparticle size from the images produced by this technique. A Hitachi SU 6600 FESEM instrument was used to obtain images of the AgNP. First the SEM was calibrated with Au on Carbon standard provided by Agar Scientific (Essex, UK). Samples were prepared by dispersing particles (1.56µg/ml) in ethanol by sonication 750 watts Ultrasonic Processor tip (Branson Ultrasonics, Ultra sonic processor VCX-750W) at 40% amplitude for a total of 45 seconds. Samples were spin coated onto pure silicon wafer which had been thoroughly cleaned by sonication in acetone for 30 minutes followed by boiling in propanol for 30 minutes. Silicon wafers were then left to air dry in a dust free environment and the nanoparticle sample was then spin coated onto the wafers 24 hours prior to measurement.

The specific area of AgNP was established with a Micrometrics GEMINI BET. BET sample holders were filled with a known mass of powdered nanoparticles and measured. The sample was degassed for 2 hours at room temperature with nitrogen gas prior to analysis. Nitrogen gas was used as the absorptive gas and a multipoint method was used in the estimation of specific surface area.

Cytotoxic evaluation

The AB and MTT assays were performed for assessment of cytotoxicity of AgNP to the three cell lines. The test used a range of eight concentrations of AgNP (3.91-500µg/ml) in which effects were likely to occur, this in turn allowed inhibitory concentration (IC_{50}) to be calculated (Murphy *et al*, 2015). In all cases results were compared to an unexposed control, eliminating any dependence of the cell line exposures on well type, seeding efficiency and numbers, exposure times and volumes. A stock suspension of AgNP (500µg/ml) was prepared aseptically from which different concentrations of nanoparticles were prepared in RPMI-1640 cell culture media followed by bath-sonication for 20 minutes (Degussa-Ney ULTRAsonik 57X, California, USA). As a positive control 10% DMSO was prepared in cell culture media. For cytotoxic analysis of nanoparticles in the presence of DPPC a concentration of 0.25µg/ml was chosen based on previous studies (Herzog *et al*, 2009). A stock solution of this test concentration (0.25µg/ml) was prepared for DPPC in RPMI-1640. Using this test concentration, a stock suspension of AgNP (500µg/ml) was prepared aseptically from which a range of nanoparticle concentrations (3.91-500µg/ml) was prepared.

Alamar Blue assay

For the AB assay, cells were seeded in 96 well microtitre plates (Nunc, Denmark) at a density of 1 x 10^5, 5 x 10^4, 4 x 10^4 and 3 x 10^4 cells/ml for 24, 48, 72 and 96hr exposures respectively in 100µl of respective media containing 10% FBS. At least three independent experiments were conducted with six replicate wells employed per concentration per plate in each independent experiment. After 24 hours of cell attachment, plates were washed with 100µl/well PBS and treated with increasing concentrations of AgNP (3.91-500µg/ml) prepared in culture media for 24, 48, 72 and 96 hours. All incubations were performed at 37°C in a 5% CO_2 humidified incubator. The assay was performed according to manufacturer's instructions. Briefly, control media and test exposures were removed, cells were rinsed with 100µl PBS and 100µl of AB solution (5% [v/v] solution of AB) prepared in fresh media with no added supplements were added to each well. After 3 hour incubation AB fluorescence was measured at excitation and emission wavelength of 531nm and 595nm respectively in a SpectraMax® M3 Microplate reader (Molecular Devices, California, USA). Wells containing AB solution and media only were used as blanks. For this assay the mean fluorescence units for six replicate cultures were calculated for each exposure treatment. Acellular studies were performed with test particles and the AB dye to confirm no interference of the particle with dye conversion (Gupta Mukherjee *et al,* 2012).

MTT assay

As with the AB assay a parallel set of three plates were set up for the MTT assay, seeded and exposed as previously described. After the same exposure times as AB assay, 24, 48, 72 and 96hr exposure or test medium was removed. Cells were washed with 100µl PBS and 100µl of freshly prepared MTT solution (5mg/ml MTT in media {without supplements}) was added to each well. After 3 hour incubation the solution was removed, cells were rinsed 100µl PBS and 100µl MTT fixative (DMSO) was added to each well. Plates were shaken at 240rpm for 10 minutes. Following this step the supernatant was removed and transferred to a new 96 well plate for analysis as it has been observed that sedimentation of AgNP on the bottom of wells interferes with absorbance readings producing higher values. Absorbance was read at 595nm in a SpectraMax® M3 Microplate reader (Molecular Devices, California, USA).

Clonogenic assay

The assay was performed in six well plates (Nunc, Denmark) each seeded with 1ml of cell suspension in media, 400 cells/ml and 1ml of media alone. Cells were allowed to attach for 12 hours to ensure there are single cells at the bottom of each well at the time of exposure. After the attachment period, wells were washed with PBS 2ml/well and then cell were treated with increasing concentrations of AgNP (3.91-500µg/ml) prepared in RPMI or AgNP prepared in RPMI with DPPC, 2ml/well. Plates were then incubated for 10 days, 37°C 5% CO_2 in a humidified incubator (Herzog *et al,* 2007; Casey *et al,* 2008). Two replicate wells on each plate were used for controls. This was performed for each test concentration. Following incubation, test exposures and control were removed and wells washed with 2ml/well PBS. Finally cells were fixed and stained with 20% carbol fuschin in dH_2O (BDH, Poole, UK) and colonies were manually counted. For all assays 10% DMSO prepared in supplemented media was used for positive control.

Reactive Oxygen Species (ROS) studies

Intracellular oxidative stress was quantified using a 2', 7'-dichlorofluorescin diacetate (DCFH-DA) plate assay to detect intracellular hydroperoxides and probe for a wide range of ROS. Confluent cells were trypsinized and seeded at a density of 1 $x10^5$ cells/ml prepared in media, onto 96 well black bottomed plates (Nunc, Denmark) and allowed to attach for 24 hours. Six independent experiments were performed with six replicate wells for control, positive control and test concentrations on each plate. A working stock of 20µM DCFH-DA in PBS was prepared and all test concentrations, positive and unexposed negative controls were prepared in this working stock and exposed to cells. The negative control consisted of 20µM DCFH-DA in PBS only and the positive control was 5µM hydrogen peroxide (H_2O_2) prepared in working stock. AgNP test concentrations (3.91-500µg/ml) and AgNP test concentrations with DPPC (0.25µg/ml) were prepared in the DCFH-DA/PBS working stock. Prior to cellular testing, acellular studies were performed with the test particles and the DCF dye at all test scenarios to confirm no reduction of the dye due to AgNP interference. No reduction of DCFH-DA by AgNP was noted.

After 24 hours of attachment, the media was removed and wells were washed with PBS, 100µl/well. Cells were then treated with 100µl of positive control, negative control and test concentrations and plates are incubated for 15min, 30 min, 1hr, 2hr, 3hr, 4hr, 5hr and 6hr. The rate of intracellular ROS production is monitored at each time point by the emission of DCFH-DA at 529nm by excitation at 504nm at the various time points (plates were re-incubated after each time point reading). Readings were performed on a SpectraMax® M3 Microplate reader (Molecular Devices, California, USA).

Inflammatory Studies

Release of inflammatory markers interleukin-8 (IL-8) and tumour necrosis factor alpha (TNF-α) were studied using Human ELISA Max™ deluxe sets for IL-8 and TNF-α of Biolegend Inc (San Diego, California). Supernatant samples were collected prior to inflammatory studies. Sample collection was performed in six well plates (Nunc, Denmark) each seeded with 1ml of cell suspension in RPMI, 5 x 10^4 cells/ml. Plates were incubated at 37°C for 24 hours. After incubation cells were treated with 1ml of increasing concentrations of AgNP (3.91-500µg/ml). Plates were incubated and cell supernatant collected at designated time intervals, 1 through 6 hours. After sample collection inflammatory studies were performed using ELISA assay as per manufactures instructions. All reagents and standards were prepared as per instructions. Absorbance was read at 450nm and 570nm within 30 minutes using a SpectraMax® M3 Microplate reader (Molecular Devices, California, USA).

Statistical analysis

At least three independent experiments were performed for each cytotoxicity endpoint. Results for each assay were expressed as a percentage of unexposed control ± standard deviation with control values set as 100%. Statistically significant differences between samples and their respective controls were calculated using the statistical analysis package InStat. Statistically significant differences were set at $p<0.05$. Normality of data was confirmed with Q-Q percentile plots and Kolmogorov-Smirnov tests. Equality of variances

was evaluated using Levène tests. One-way analysis of variances (ANOVA) followed by Dunnett's multiple comparison tests were carried out for normally distributed samples with homogeneous variances. Non-parametric tests, namely Kruskal-Wallis followed by Mann-Whitney-u-tests were applied to samples without normal distribution and/or inhomogeneous variances. Cytotoxicity data (where appropriate) was fitted to a sigmoidal curve and a four parameter logistic model used to calculate the Inhibitory Concentration (IC_{50}) values. The IC_{50} value refers to a concentration of a compound where a 50% effect is observed in this case a reduction in cell viability. IC_{50} values were reported as ±95% confidence intervals. IC_{50} values were estimated using XLfit3™, a curve fitting add on for Microsoft® Excel (ID Business Solutions, UK).

Results

Particle characterization

The particles utilized in this study (PVP coated, Sigma-Aldrich, Ireland) were characterized using SEM analysis (figure 1) which demonstrated spherical particles with an average size of 50-70nm. The size is representative of pristine particles as purchased suspended in dH_2O. For more detailed sizing analysis DLS was used to provide a rough overview of particle interaction with different biological media providing a more realistic view of how AgNP will be presented to cells and give insight into the response they may produce.

Figure 2 demonstrates DLS measurements on AgNP suspended in dH_2O, in RPMI cell culture media and in the presence of DPPC. A representative concentration of AgNP (15.6µg/ml) that produces a biological effect was chosen. Two peaks are demonstrated in analysis of AgNP alone with the greatest number of particles falling in the range of 34nm ±3.5. The broader peak can be attributed to particle agglomeration. A slight shift in hydrodynamic diameter was observed in preparations of AgNP in RPMI. Dispersed in RPMI alone two clear peaks were observed one representing RPMI itself and the other at approximately 40nm representing AgNP. The addition of DPPC causes little change in hydrodynamic diameter but produces a larger peak at the 20-40nm range suggesting possible isolation of particles from larger agglomerates with its addition to the system.

While DPPC appears to have no influence on particle size the data indicate an influence on particle agglomeration. As such UV-vis absorption was performed to determine any interaction between the various components of the different suspensions. No interaction between components was demonstrated indicating that a secondary toxicity due to depletion of nutrients would be unlikely.

Zeta potential analysis was performed on the same particle suspensions as used for sizing analysis and demonstrates the overall stability of the system. A system is unstable when values fall within the range of 30mV to -30mV. It was noted that AgNP suspended in dH_2O fell within this range, less than 30mV, indicating particles were unstable an unusual result as particles are PVP coated. When suspended in cell culture media and in the presence of DPPC the system was stable. The addition of DPPC was noted to have no impact on the overall stability.

Cytotoxicity Testing

The cytotoxicity of AgNP on A549 cells was assessed using the viability assays MTT, Alamar blue (AB) and a DCF-DA plate assay to detect intracellular oxidative stress. The influence of DPPC on the observed toxicity was investigated using the same array of toxicological assays. A positive control of 10% DMSO was employed for all viability assays and 5μM H_2O_2 was employed for ROS studies. The ability of AgNP to induce an inflammatory response and the impact of DPPC on this response was also investigated using ELISA based assays for the detection of IL-8 and TNF-α release. Cytotoxicity data for AgNP exposure is presented in table 1. The results of the MTT assay are presented for toxicity testing in the presence and absence of DPPC. Both MTT and AB assays were performed. Results for AB assay not shown, data is represented in table 1.

Figure 3 represents the cytotoxic response of A549 cells to AgNP exposure as determined by the MTT assay. Reduction in cell viability due to exposure occurred in a dose and time dependent manner. A significant reduction in mitochondrial integrity was observed after 48 hours at all AgNP concentrations. Significant reduction after 72 and 96 hour exposures was noted at concentrations of 15.6μg/ml and above compared to the unexposed control, while a significant reduction in cell survival at all exposure times occurred at 31.25μg/ml and above.

A DCF-DA plate assay was employed to detect any ROS production in response to AgNP exposure over a 6 hour period with readings taken every hour. This study indicated no intracellular ROS production in response to exposure to AgNP. The generation of intracellular hydro peroxides was noted at the highest concentration 500μg/ml with production increasing in a time dependant manner. Induction of ROS was first detected at this concentration after 15 minutes, with the highest induction observed after 1 hour. Results are not shown.

The ability of DPPC to influence toxicity was investigated using the same array of cyto-toxicological tests.

Figure 4 displays the toxic response of A549 cells to AgNP in the presence of 0.25μg/ml DPPC. A dose dependant response to AgNP exposure was observed. A change in toxicity was not noted, however the pattern appeared altered in the presence of DPPC. A short delay in toxicity between 48 and 72 hours was observed after which a significant reduction in cell viability occurred. Significant reduction in cell survival to all exposure concentrations was noted after 72 hours. After 24 hours, significant loss in cell viability was observed at a concentration of 15.6μg/ml with a significant decline at 7.8μg/ml and above following 96 hour exposure. Significant cell death compared to the unexposed control at all exposure intervals was observed at 62.5μg/ml and above. The addition of DPPC may alter the pattern of toxicity by causing a delay in toxicity in the first 48 hours, after which a significant reduction in viability is observed at 72 hours.

The delay and increase in viability at lower nanoparticle concentrations at 48 hours may result from surviving cells beginning to replicate. DPPC is a surfactant and as such will associate with the nanoparticles surface. This association may result in a "Trojan horse" effect or delayed toxicity as observed at lower concentrations in the first 48 hours. After this time it is possible the DPPC coating has been removed following nanoparticle entry to the cell and trafficking to various cellular compartments allowing the naked nanoparticle to exert its toxic effects (Wang *et al*, 2013)**.**

In addition to cytotoxic evaluation, the clonogenic assay was performed to analyse the effect of longer exposures to AgNP. This assay was performed over a 10 day exposure period and monitored the ability of cells to form colonies in the presence of AgNP. The ability of cells to

proliferate following AgNP exposure with the addition of DPPC was significantly reduced compared to the unexposed control. This was observed at all exposure concentrations. It was found that the ability of A549 cells to proliferate was inhibited at the lowest concentration of 3.91µg/ml and above with no colony formation and therefore no cell survival at concentrations of 62.5µg/ml and above, as shown in Figure 5. Interestingly it appeared that the addition of DPPC increased the toxicity of Ag nanoparticles towards cells with significant reductions in colony formation compared with exposure to AgNP alone.

A DCF-DA plate assay was employed to investigate the effect of DPPC on ROS generation in A549 cells following AgNP exposure. From the data it appeared that in the presence of DPPC there was increased generation of intracellular ROS from a dose of 31.25µg/ml and above. Figure 6 illustrates ROS production in a dose and time dependant manner. Induction was detected at concentrations as low as 31.25µg/ml after 15 minutes exposure, with maximum production noted at 500µg/ml after 30 minutes. ROS production was detected up to 6 hours after initial exposure at a concentration of 500µg/ml and up to 4 hours after initial exposure at 250µg/ml. Significant increases were noted at doses of 62.5µg/ml after 30 minutes, 125µg/ml after 15 and 30 minute exposures and at higher doses significant generation was observed from 15 to 30 minutes and 2 to 3 hours at 250µg/ml and at 15 minutes to 5 hours at 500µg/ml. From the data it is clear that the presence of DPPC mediates oxidative stress in A549 cells by increasing intracellular ROS formation following AgNP exposure.

Inflammatory Studies

The ability of AgNP to induce IL-8 and TNF-α production and the effect of the addition of DPPC was investigated using ELISA based assays.

Figure 7 demonstrates IL-8 release following exposure to AgNP. At the highest concentration, 50µg/ml, production of IL-8 was observed after 2 hours. Levels were shown to decline after 3 hours with a second peak in levels demonstrated after 4 hours. The lower dose of AgNP caused IL-8 release initially after exposure with increasing generation up to 2 hours after exposure. A similar reduction in levels was detected at 3 hours after which an increase in IL-8 was detected at 4 and 6 hours. A significant increase in IL-8 compared to the unexposed control was noted at 2, 3, 4 and 6 hours at a concentration of 50µ/ml and at all time intervals at 25µg/ml. The data suggest that at sub-lethal levels of AgNP, 25µg/ml, a more immediate and long lived inflammatory response is initiated compared to higher toxic doses.

Figure 8 represents IL-8 release in A549 cells following AgNP exposure with the addition of DPPC. The data show that the presence of DPPC alters the pattern of IL-8 release in cells. The levels of IL-8 detected were substantially higher than exposure to AgNP alone and production occurs at a faster rate with greater levels detected after 1 hour exposure. Similar to figure 7 a second spike in release was detected at 6 hours. The presence of DPPC generated an immediate and prolonged inflammatory response compared to exposure to AgNP alone as illustrated by IL-8 levels detected at 1 and 6 hours. Significant release was noted at 1, 2, 3 and 6 hours for all doses compared to the unexposed control. While DPPC leads to an enhanced production of IL-8, the pattern appears not to be dependent on concentration suggesting that regardless of AgNP dose the same biological response is initiated.

Figure 9 illustrates TNF-α release following AgNP exposure. Generation of TNF-α at a dose of 25µg/ml was immediate and short lived with peak levels detected after 1 hour and a rapid reduction observed at 2 hours and above. A similar pattern was detected at the highest dose

with high levels detected after 1 hour followed by a swift decline. However as demonstrated with IL-8, a second spike in TNF-α levels occurs at 6 hours. Significant TNF-α release was detected after 1 hour following 25µg/ml exposure and after 1, 2, 3 and 6 hours after 50µg/ml exposure.

In the presence of DPPC (figure 10) substantially lower levels of TNF-α were released compared to AgNP alone. TNF-α was generated after 1 hour exposure with a decline in levels detected after at 2 hours. Unlike exposure to AgNP alone, the second increase in levels was detected at 3 hours and gradually increased with time. Significant increases in TNF-α release were noted at 1, 3, 4 and 6 hours at a dose of 50µg/ml and at 1, 4 and 6 hours at 25µg/ml. It appears the presence of DPPC produces a prolonged inflammatory response similar to that observed with IL-8 release. The addition of DPPC also modifies the pattern of TNF-α release, which similar to IL-8, is not dependent on AgNP concentration.

Discussion

It is apparent from the literature that exposure to nanoparticles is becoming more widespread mainly through their continued incorporation into consumer products. As a result there is an increasing incidence of direct contact between nanoparticles and biological systems. This growing concern of nanoparticle exposure highlights the need for a complete and thorough toxicological investigation to determine what effects are induced and what factors within biological systems play a role in the resulting effects.

The physiochemical characteristics of AgNP play an important role in how they will interact with biological systems. Primarily the size and associated surface area, shape and chemical composition have all been shown to be of great importance to nanoparticle toxicity and must be considered when interpreting toxicological data (Sur *et al*, 2012; Warheit, 2007). As well as nanoparticle characteristics, the influence of ion release on toxicity must also be considered and further investigation is required to determine how much toxicity can be attributed to ions and the particle itself (Beer *et al*, 2012; Navarro *et al*, 2008; Kim *et al*, 2009). In this instance a thorough characterization of nanoparticles was undertaken yielding a size of 34nm ± SD 3.5 and no interaction between components was evident. Despite this, the effect individual components play on resulting toxicity must be considered as physiochemical characterization can never truly represent interactions occurring *in vitro* or *in vivo*.

Table 1 displays cytotoxic data for both viability assays. The AB assay demonstrates an increase in IC_{50} values at 72 and 96 hours. This assay has multiple sites of conversion within the cell and thus gives an indication into both viability and general cell function. As such the increase in cell viability observed may be attributed to cell recovery. The A549 cell line has a doubling time of 22 hours and it is possible that after the first 48 hours of exposure where toxicity is observed any surviving cells begin to replicate again slowly resulting in an increase in IC_{50} values. This was also observed at 96 hours with the addition of DPPC. In the MTT assay which is indicative of mitochondrial integrity only, a time dependant reduction in values was observed. Exposure to AgNP was also noted to induce an inflammatory response with release of IL-8 and TNF-α. The presence of DPPC significantly altered the levels of release induced by exposure on A549 cells. The difference in levels released when DPPC was present compared to AgNP exposure alone was found to be statistically ($p<0.05$) significant at all exposure concentrations and time points.

The mechanism of cell death caused by AgNP can be related to oxidative stress. Mitochondrial cell death by ROS generation has been described in a number of studies as the primary mechanism of nanoparticle related cell death with its generation forming a critical step in initiation of apoptotic pathways (Martindale & Holbrook, 2002; Sastre *et al*, 2000; Piao *et al*, 2011). ROS are generated under normal physiological conditions and are continually eliminated by naturally occurring antioxidants. Under certain "stressful" conditions cells are unable to maintain homeostasis as increased quantities of ROS are produced which overwhelm the antioxidant systems (Arora *et al*, 2008; Piao *et al*, 2011). Previous studies have shown that AgNP not only induce ROS but can also inhibit antioxidants such as glutathione (Arora *et al*, 2008; Hussain *et al*, 2005; Chairuangkitti *et al*, 2013; Piao *et al*, 2011). This process may be in part due to lipid peroxidation caused by nanoparticle exposure. AgNP and ZnO have been identified as a cause of lipid peroxidation enhancing ROS production while also quenching naturally occurring antioxidants (Premanathan *et al*, 2011; Adeyemi & Faniyan, 2014). This response induces downstream dysfunction such as inflammation and DNA damage within the cell culminating in cell death (Nel *et al*, 2006). While mitochondrial involvement appears to be the mechanism of cell death, other pathways have been hypothesised. Death via a ROS-independent pathway has also been observed in A549 cells following exposure to AgNP. This results in cell cycle arrest rather than cell death by interfering with a regulatory protein critical in progression of the cell cycle (Chairuangkitti *et al*, 2013)**.** This may partially explain the lack of ROS induction observed following AgNP exposure but with a reduction in viability still evident. Cells may be arrested at various stages of the cell cycle without the involvement of ROS following AgNP exposure as demonstrated in the data.

The induction of oxidative stress is a critical step in the biological response to nanoparticle exposure and causes a number of cellular implications including an enhanced inflammatory response. Excessive ROS production leads to activation of a number of pro-inflammatory cytokines including IL-8 and TNF-α and within the lung which have been implicated in certain respiratory disorders (Henricks & Nijkamp, 2001; Zuo *et al*, 2013). IL-8 is involved in the activation and migration of cells such as neutrophils, during acute inflammation. It can also up-regulate adhesion molecules involved in adherence and migration of cells through the endothelium (Feghali & Wright, 1997; Lim *et al*, 2012). The lung epithelium in particular is an important source of IL-8 and as such is a key player in the mediation of lung inflammation (Donaldson *et al*, 1998). IL-8 has been the focus of a number of studies related to nanoparticle toxicity, with its release implicated in the recruitment of inflammatory cells to the lung (Singh *et al*, 2007). Specifically, following AgNP exposure, significant release of IL-8 from macrophages has been demonstrated, with both particle size and the generation of ROS playing a crucial role in its release (Lim *et al*, 2012; Park *et al*, 2011).

TNF-α is a potent cytokine involved in the initiation and maintenance of inflammation (Nathan, 2002). TNF-α can mediate a number of responses directly such as fever and, tissue damage, as well as causing indirect effects by downstream signalling leading to the activation of other inflammatory factors including IL-6 (Feghali & Wright, 1997; Warren, 1990). This cytokine has been implicated in the development of pulmonary fibrosis following silica micro-particle exposure causing increased endothelial permeability to macromolecules as well as its up-regulation following exposure to various nanoparticles (Napierska *et al*, 2012; Henning *et al*, 1997; Pryhuber *et al*, 2003; Piguet *et al*, 1990). The detection of increased levels of both IL-8 and TNF-α following exposure implicates AgNP in the inflammatory process with an augmented response observed following the addition of DPPC. The increased levels of IL-8 in particular correlates to the ROS generation observed following its addition. In the case of IL-8, an immediate release is observed in the presence of DPPC and its early release has been

proposed as a potential bio-marker for acute inflammation in relation to AgNP exposure which the data presented here supports (Lim *et al*, 2012; Park *et al*, 2011).

The ability of the DPPC to increase and prolong the activation of both cytokines compared to AgNP alone suggests progression from acute to chronic inflammation. It has been proposed that high levels coupled with sustained release of these cytokines may prevent resolution resulting in the development of chronic inflammation. It was observed that in certain cases it was not the highest AgNP concentration that generated the greatest release of cytokines. This is not surprising as high concentrations can cause cells to enter a death process whereas lower concentrations can induce an inflammatory. Lim *et al* demonstrated cytokine gene expression at sub lethal concentrations of AgNP, in particular IL-8 release at 2.5µg/ml (Lim *et al*, 2012).

DPPC is a major component of lung surfactant produced by type II alveolar cells, similar to A549 cells, and as such has been used as a surfactant model in numerous toxicity studies (Kumar & Bohidar, 2010; Dobbs *et al*, 1987; Foucaud *et al*, 2007; Porter *et* al, 2008; Sager *et al*, 2007). Employed as a particle coating, DPPC has been shown to exert a protective effect preventing degradation and allowing controlled release of encapsulated drug compounds; however there is increasing evidence of its contribution to toxicity and induction of oxidative stress (Kaviratna & Banerjee, 2009; Herzog *et al*, 2009; Foucaud *et al*, 2007; Hamilton Jr *et al*, 2008). The data highlight the importance of ROS in cell toxicity particularly in the presence of DPPC. DPPC appears to increase oxidative stress within the cell in agreement with other studies where it was also found that its addition significantly increased ROS production in A549 cells (Herzog *et al*, 2009; Foucaud *et al*, 2007). An investigation into different variations of silica nanoparticles including iron- and titania- containing particles, noted increased levels of intracellular ROS generation. This was believed to occur through nanoparticle entry by a Trojan-horse type mechanism dependant on surface chemistry of the particles (Limbach *et al*, 2007). A similar theory can be applied to this study and the increased oxidative stress observed following the addition of DPPC. It is possible that interaction with DPPC causes particles to have a higher level of dispersion, increasing the surface area available for interaction and therefore increasing the likelihood of cellular uptake - resulting in generation of ROS. It must also be considered that the surface chemistry and activity of particles is altered by DPPC, changing its toxicity, making the particles more reactive and thus more toxic (Herzog *et al*, 2009; Hamilton Jr *et al*, 2008; Buford *et al*, 2007).

The observation that cell death can occur via a number of pathways in A549 cells indicates a two tiered mechanism of cell death, cell cycle arrest and ROS mediated mitochondrial dependant cell death (Piao *et al*, 2011). The data in this study suggest that while not changing nanoparticle toxicity DPPC may influence death pathways as demonstrated by the induction of oxidative stress. The observation that DPPC leads to ROS generation in A549 cells suggests a possible switching from a ROS independent pathway as described by Chairuangkitti *et al*, 2013 causing cell cycle arrest to a ROS dependent pathway culminating in apoptotic cell death (Chairuangkitti *et al*, 2013). Further mechanistic studies are required to conclusively determine if pathway switching due to DPPC interaction is occurring.

Conclusion

This study has demonstrated the role of DPPC in modifying toxicity, namely inducing intracellular ROS production. Its interaction with AgNP highlights the importance of particle-surfactant interactions and the altered effects produced when in contact with mammalian cells. The data presented are in agreement with previous studies illustrating the impact on toxicity

caused by nanoparticle contact with DPPC and the resulting alteration in ROS generation and inflammatory response. These findings may contribute to developing a realistic risk assessment of nanoparticle exposure and the potential biological outcomes following entry and interaction with various fluids and surfactants present in the body.

Acknowledgements

This work is funded by the Science foundation Ireland's Research Frontiers Programme and Fiosraigh Scholarship Programme. This work was conducted under the framework of the INSPIRE programme, funded by the Irish Government's Programme for Research in Third Level Institutions, Cycle 4, National Development Plan 2007-2013, supported by the European Union Structural Fund.

Conflict of Interest

The authors declare there are no conflicts of interest.

References

Adeyemi O. S, Faniyan T. O. 2014. Antioxidant status of rats administered silver nanoparticles orally. *J Taibah Univ Med Sci.* **9:** 182-186

Aggarwal P, Hall J. B, McLeland C. B, Dobrovolskaia M. A, McNeill S. E. 2009. Nanoparticle interaction with plasma proteins as it relates to particle biodistribution, biocompatibility and therapeutic efficacy. *Adv Drug Deliver Rev*. **16:** 428-437

Arora J. J, Rajwade J. M, Paknikar K. M. 2008. Cellular responses induced by silver nanoparticles: In vitro studies. *Toxicol Lett.* **179:** 93-100

Bakshi M. S, Zhao L, Smith R, Possmayer F, Petersen N. O. 2008. Metallic nanoparticle pollutants interfere with pulmonary surfactant function in vitro. *Biophys J*. **94:** 855-868

Beer C, Foldjerg R, Hayashi Y, Sutherland D. S, Autrup H. 2012. Toxicity of silver nanoparticles-nanoparticle or silver ion? *Toxicol Lett.* **208:** 286-292

Bouwmeester H, Dekkers S, Noordam M.Y, Hagens W. I, Bulder A. S, de Heer C, ten Voorde S. E, Wijnhoven S. W, Marvin H. J, Sips A. J. 2009. Review of health safety aspects of nanotechnologies in food production. *Regul Toxicol Pharmacol*. **53:** 52-62

Buford M. C, Hamilton Jr R. F, Holian A. 2007. A comparison of dispersing media for various engineered carbon nanoparticles. *Part Fibre Toxicol.* **4:** 6

Casey A, Herzog E, Lyng F. M, Byrne H. J, Chambers G, Davoren M. 2008. Single walled carbon nanotubes induce indirect cytotoxicity by medium depletion in A549 lung cells. *Toxicol Lett.* **179:** 78-84

Chairuangkitti P, Lawanprasert S, Roytrakul S, Aueviriyavit S, Phummiratch D, Kulthong K, Chanvorachote P, Maniratanachote R. 2013. Silver nanoparticles induce toxicity in A549 cells via ROS-dependent and ROS-independent pathways. *Toxicol In Vitro*. **27:** 330-338

Dobbs L. G, Wright J.R, Hawgood S, Gonzalez R, Venstrom K, Nellenbogen J. 1987. Pulmonary surfactant and its components inhibit secretion of phosphatidylcholine from cultured rat alveolar type II cells. *Proc Natl Acad Sci USA.* **84:** 1010-1014

Donaldson K, Li X. Y, MacNee W. 1998. Ultrafine (nanometer) particle mediated lung injury. *J Aerosol Sci.* **29:** 553-560

Ehrenberg M. S, Friedman A. E, Finkelstein J. N, Oberdorster G, McGrath J. L. 2009. The influence of protein absorption on nanoparticle association with cultured endothelial cells. *Biomaterials.* **30:** 603-610

Feghali C. A, Wright T. M. 1997. Cytokines acute and chronic inflammation. *Front Biosci.* **2:** 12-26

Foucaud L, Wilson M. R, Brown D. M, Stone V. 2007. Measurement of reactive species production by nanoparticles prepared in biologically relevant media. *Toxicol Lett.* **174:** 1-9

Gupta Mukherjee S, O'Claonadh N, Casey A, Chambers G. 2012. Comparative *in vitro* cytotoxicity study of silver nanoparticle on two mammalian cell lines. *Toxicol In Vitro*. **26**: 238-251

Hamilton Jr R. F, Thakur S. A, Holian A. 2008. Silica binding and toxicity in alveolar macrophages. *Free Rad Biol Med.* **44:** 1246-1258

Henning B, Goldblum S. E, McClain C. J. 1987. Interleukin 1 (IL-1) and tumour necrosis factor/cachectin (TNF) increase endothelial permeability in vitro. *J Leukoc Biol.* **42:** 551-552

Henricks P. A. J, Nijkamp F. P. 2001. Reactive oxygen species as mediators in asthma. *Pulm Pharmacol Ther.* **14:** 409-421

Herzog E, Byrne H. J, Davoren M, Casey A, Duschl A, Oostingh G. J. 2009. Dispersion medium modulates oxidative stress response of human lung epithelial cells upon exposure to carbon nanomaterial samples. *Toxicol Appl Pharm.* **236:** 276-281

Herzog E, Casey A, Lyng F. M, Chambers G, Byrne H. J, Davoren M. 2007. A new approach to the toxicity testing of carbon based nanomaterials – the clonogenic assay. *Toxicol Lett.* **174:** 49-60

Hussain S. M, Hess K. L, Gearhart J. M, Geiss K. T, Schlager J. J. 2005. In vitro toxicity of nanoparticles in BRL3A rat liver cells. *Toxicol In Vitro.* **19:** 975-983

Kaviratna A. S, Banerjee R. 2009. The effects of acids on dipalmitoylphosphatidylcholine (DPPC) monolayers and liposomes. *Colloid Surface A.* **345:** 155-162

Kim S, Choi J. E, Choi J, Chung K. H, Park K, Yi J, Ryu D. Y J. 2009. Oxidative stress dependent toxicity of silver nanoparticles in human hepatoma cells. *Toxicol In Vitro.* **23:** 1076-1084

Kumar P, Bohidar H. B. 2010. Aqueous dispersion stability of multi-carbon nanoparticles in anionic, cationic, neutral, bile salt and pulmonary surfactant solutions. *Colloid Surface A.* **361 (1-3):** 13-24

Lim D-H, Jang J, Kim S, Kang T, Lee K, Choi I-H. 2012. The effects of sub-lethal concentrations of silver nanoparticles on inflammatory and stress genes in human macrophages using cDNA microarray analysis. *Biomaterials.* **33:** 4690-4699

Limbach L. K, Wick P, Manser P, Grass R. N, Bruinink A, Stark W. J. 2007. Exposure of engineered nanoparticles to human lung epithelial cells: influence of chemical composition and catalytic activity on oxidative stress. *Environ Sci Technol.* **41:** 4158-4163

Liu H, Yang D, Yang H, Zhang H, Zhang W, Fang Y, Lin Z, Tian L, Lin B, Yan J, Xi Y. 2013. Comparative study of respiratory tract immune toxicity induced by three sterilisation nanoparticles: silver, zinc oxide and titanium dioxide. *J Hazard Mater.* **248-249:** 478-486

Martindale J. L, Holbrook N. J. 2002. Cellular response to oxidative stress: signalling for suicide and survival. *J Cell Physiol.* **192:** 1-15

Medicinenet, Med terms Medical Dictionary. Define biofluid. Retrieved on 8th August, 2014 from http://www.medterms.com/script/main/art.asp?articlekey=38690

Misra S. K, Dybowska A, Berhanu D, Luoma S. L, Valsami-Jones E. 2012. The complexity of nanoparticle dissolution and its importance in nanotoxicological studies. *Sci Total Environ.* **438:** 225-232

Murphy A, Sheehy K, Casey A, Chambers G. 2015. Potential of Biofluid components to modify Silver Nanoparticle Toxicity. *J Appl Toxicol.* DOI: 10.1002/jat.3132

Mwilu S.K, El Badawy A.M, Bradham K, Nelson C, Thomas D, Scheckel K. G, Tolaymat T, Ma L, Rogers K. R. 2013. Changes in silver nanoparticles exposed to human synthetic stomach fluid: Effects of particle size and surface chemistry. *Sci Total Environ.* **447:** 90-98

Napierska D, Thomassen L. C. J, Vanaudenaerde B, Luyts K, Lison D, Martens J. A, Nemery B, Hoet P. H. M. 2012. Cytokine production by co-cultures exposed to monodisperse amorphous silica nanoparticles: The role of size and surface area. *Toxicol Lett.* **211:** 98-104

Nathan C. 2002. Points of control of inflammation. *Nature.* **420:** 846-852

Navarro E, Piccapietra F, Wagner B, Marconi F, Kaegi R, Odzak N, Sigg L, Behra R. 2008. Toxicity of silver nanoparticles to *Chlamydomonas reinhardtii. Environ Sci Technol.* **42:** 8959-8964

Nel A, Xia T, Madler L, Ning L. 2006. Toxic potential of materials at the nanolevel. *Science.* **311:** 622-627

Park J, Lim D-H, Lim H-J, Kwon T, Choi J-S, Jeong S, Choi I-H, Cheon J. 2011. Size dependant macrophage responses and toxicological effects of Ag nanoparticles. *Chem Comm.* **47:** 4382-4384

Piao M. J, Kang K. A, Lee I. K, Kim H. S, Kim S, Choi J. Y, Choi J, Hyun J. W. 2011. Silver nanoparticles induce oxidative cell damage in human liver cells through inhibition of reduced glutathione and induction of mitochondria-involved apoptosis. *Toxicol Lett*. **201:** 92-100

Piguet P. F, Collart M.A, Grau G. E, Sappino A. P, Vassalli P. 1990. Requirement of tumour necrosis factor for development of silica-induced pulmonary fibrosis. *Nature.* **344:** 245-247

Porter D, Sriram K, Wolfarth M, Jefferson A, Schwegler-Berry D, Andrew M. E, Castranova V. 2008. A biocompatible medium for nanoparticle dispersion. *Nanotoxicology.* **2:** 144-154

Premanathan M, Karthikayan K, Jeyasubramanian K, Manivannan G. 2011. Selective toxicity of ZnO nanoparticles toward Gram-positive bacteria and cancer cells by apoptosis through lipid peroxidation. *Nanomed-Nanotechnol*. **7:** 184-192

Pryhuber G. S, Huyck H. L, Baggs R, Oberdorster G, Finkelstein J.N. 2003. Induction of chemokines by low-dose intratracheal silica is reduced by TNFR-1 (p55) null mice. *Toxicol Sci.* **72:** 150-157

Sager T. M, Porter D.W, Robinson V. A. 2007. Improved method to disperse nanoparticles for in vitro and in vivo investigation of toxicity. *Nanotoxicology.* **1:** 118-129

Sastre J, Pallardó F. V, Viña J. 2000. Mitochondrial oxidative stress plays a key role in aging and apoptosis. *IUBMB Life.* **49:** 427-435

Serrano A. G, Perez-Gil J. 2006. Protein-lipid interactions and surface activity in the pulmonary surfactant system. *Chem Phys Lipids.* **114:** 105-118

Shum P, Kim J. M, Thompson D.H. 2001. Phototriggering of liposomal drug delivery systems. *Adv Drug Deliv*. **53:** 273-284

Singh S, Shi T, Duffin R, Albrecht C, Van B. D, Hohr D, Fubini B, Martra G, Fenoglio I, Borm P. J, Schins R. P. 2007. Endocytosis, oxidative stress and IL-8 expression in human lung epithelial cells upon treatment with fine and ultrafine TiO_2: role of the specific surface area and of surface methylation of the particles. *Toxicol Appl Pharmacol.* **222:** 141-151

Sozar N, Kokini J.L. 2009. Nanotechnology and its applications in the food sector. *Trends Biotechnol*. **27:** 82-9

Srinivas A, Jaganmohan Rao P, Selvam G, Balakrishna Murthy P, Neelakanta Reddy P. 2010. Acute inhalation toxicity of cerium oxide nanoparticles in rats. *Toxicol Lett.* **205:** 105-115

Sur I, Altunbek M, Kahraman M, Culha M. 2012. The influence of the surface chemistry of silver nanoparticles on cell death. *Nanotechnology.* **23:** 1-12

Varez-Lorenzo C, Bromberg L, Concheiro A. 2009. Light-sensitive intelligent drug delivery systems. *Photochem Photobiol.* **85:** 848-860

Wang F, Yu L, Monopoli M.P, Sandin P, Mahon E, Salvati A, Dawson K. A. 2013. The biomolecular corona is retained during nanoparticle uptake and protects the cells form the damage induced by cationic nanoparticles until degraded in lysosomes. *Nanomed-Nanotechnol.* **9:** 1159-1168

Warheit D. B. 2007. How meaningful are the results of nanotoxicity studies in the absence of adequate material characterization. *Toxicol Sci.* **101:** 183-185

Warren J. S. 1990. Interleukins and tumour necrosis factor in inflammation. *Crit Rev Clin Lab Sci.* **28:** 37-59

Yavlovich A, Singh A, Blumenthal R, Puri A. 2011. A novel class of photo-triggerable liposomes containing DPPC:$DC_{8,9}$PC as vehicles for delivery of doxorubicin to cells. *BBA-Biomembranes.* **1808:** 117-126

Zuo L, Otenbaker N. P, Rose B. A, Salisbury K. S. 2013. Molecular mechanisms of reactive oxygen species-related pulmonary inflammation and asthma. *Mol Immunol.* **56:** 57-63

Table 1 Calculated IC_{50} values (µg/ml) resulting from exposure to AgNps for the AB and MTT assays in the A549 cell line. ** Denotes where a 50% effect was not observed. IC_{50} values were calculated from the average response of three independent experiments fitted to a sigmoidal curve and a four parameter logistic model used to calculate Inhibitory Concentration (IC_{50}) with a ($p<0.05$)

Cell Line	AB Assay IC_{50} (µg/ml)				MTT Assay IC_{50} (µg/ml)			
	24hr	48hr	72hr	96hr	24hr	48hr	72hr	96hr
A549	116.23	11.68	39.86	118.4	340	115	116	91
A549 + DPPC	46.06	45.3	41.78	96.84	**	**	49	80

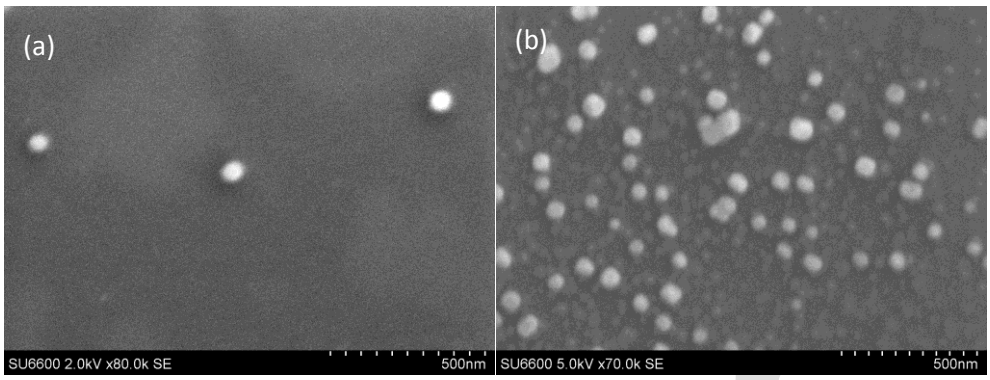

Figure 1 SEM micrograph at scale bar of 500nm image pristine AgNP (a) at magnification of x80,000 and (b) at a magnification of x70,000 dispersed in ethanol to a concentration of 1.56µg/ml by sonication using Ultrasonic Processor tip.

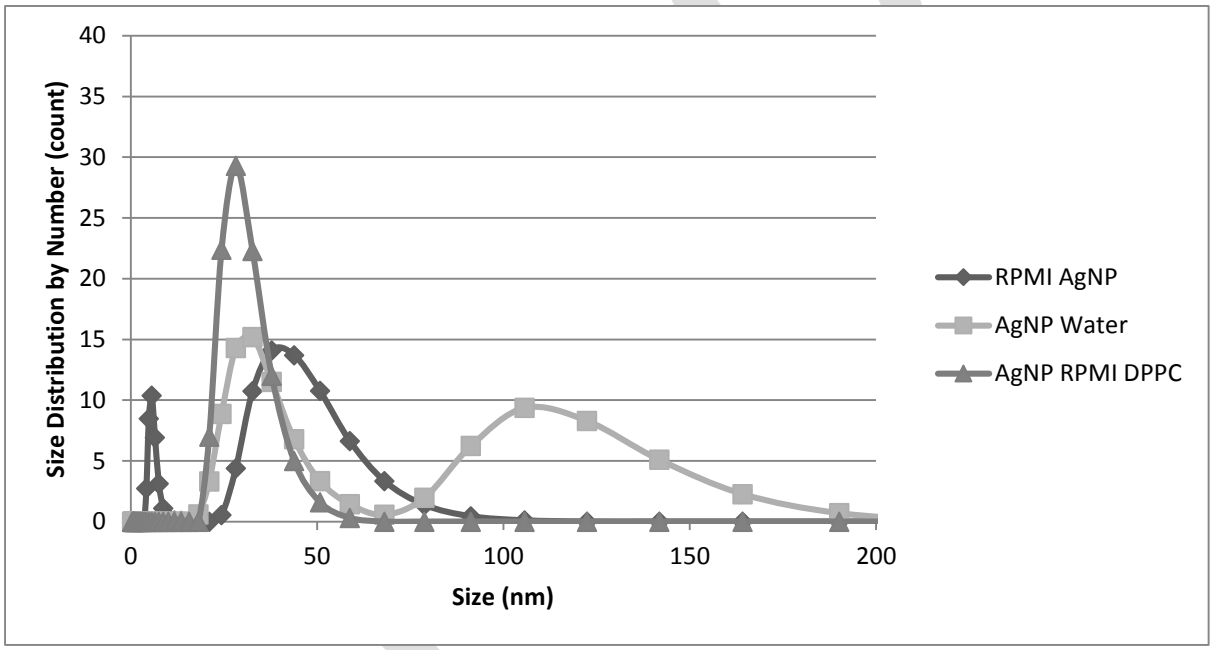

Figure 2 Dynamic Light Scattering size (nm) particle number distribution plot of AgNP (15.6µg/ml) dispersed in media, dH_2O and in the presence of DPPC. Data presented is the average of three individual experiments

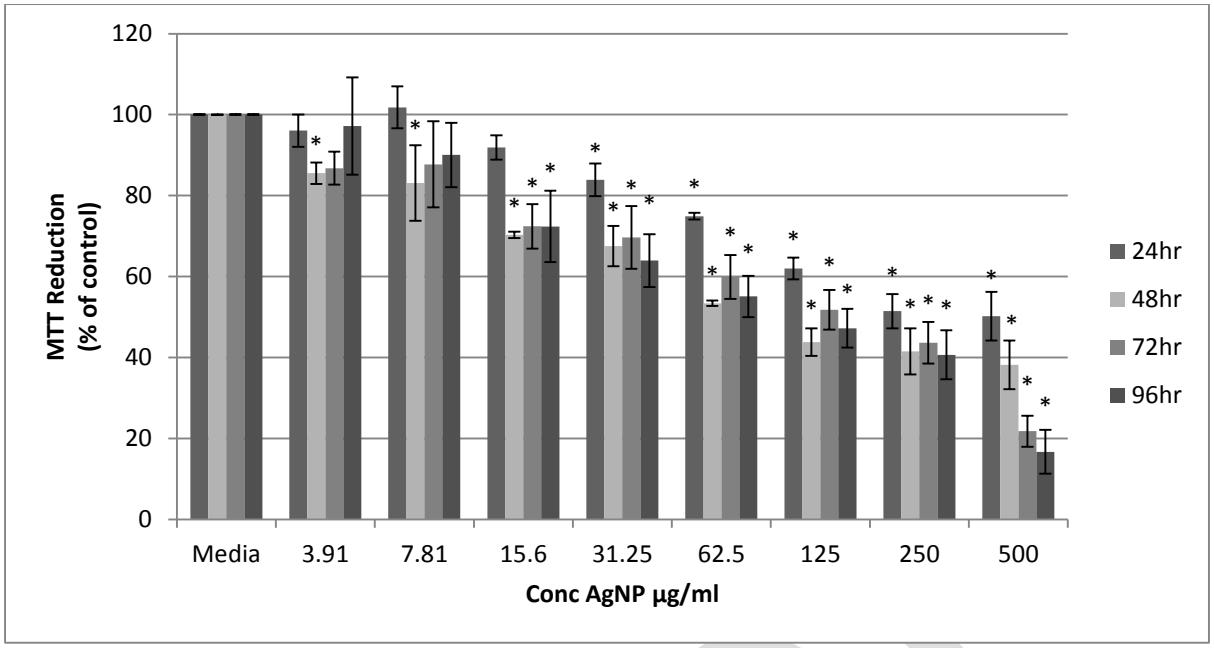

Figure 3 Cytotoxicity of AgNP in A549 cells after 24, 48, 72 and 96hr exposure as determined by the MTT assay. Data expressed as percentage of control mean ± SD of three individual experiments. * denotes a statistically significant ($p < 0.05$) difference from the unexposed control

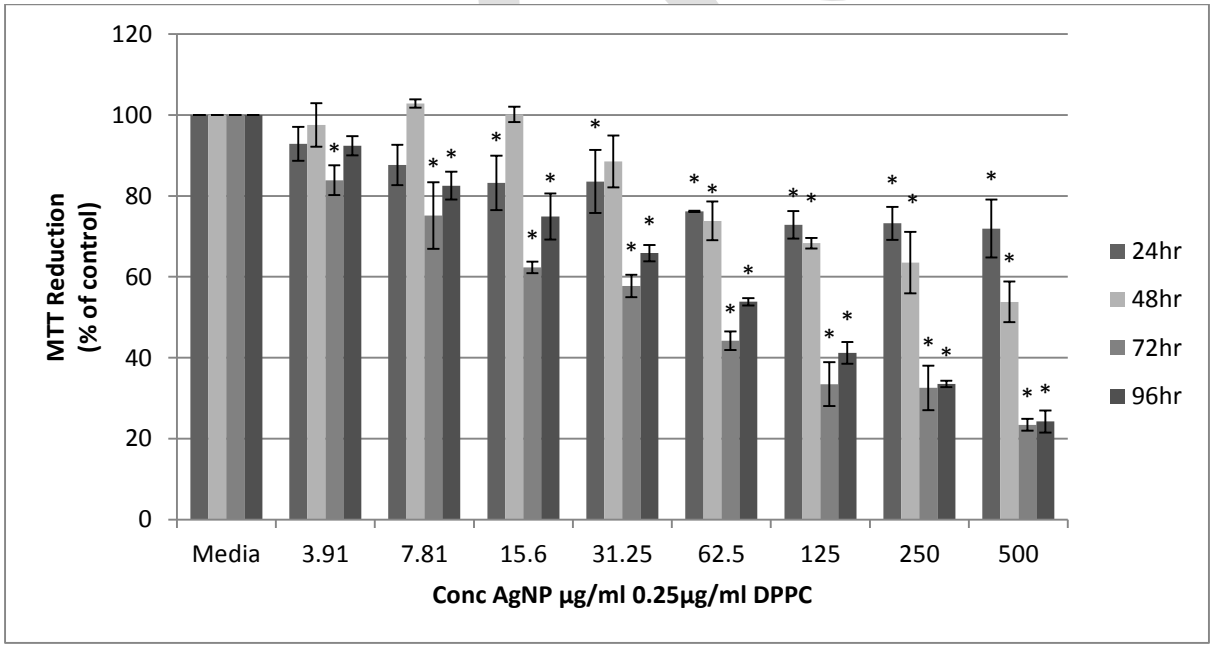

Figure 4 Cytotoxicity of AgNP in A549 cells with added DPPC after 24, 48, 72 and 96 hour exposures as determined by the MTT assay. Data expressed as percentage of control mean ± SD of three independent experiments. * denotes a statistically significant ($p < 0.05$) difference from the unexposed control

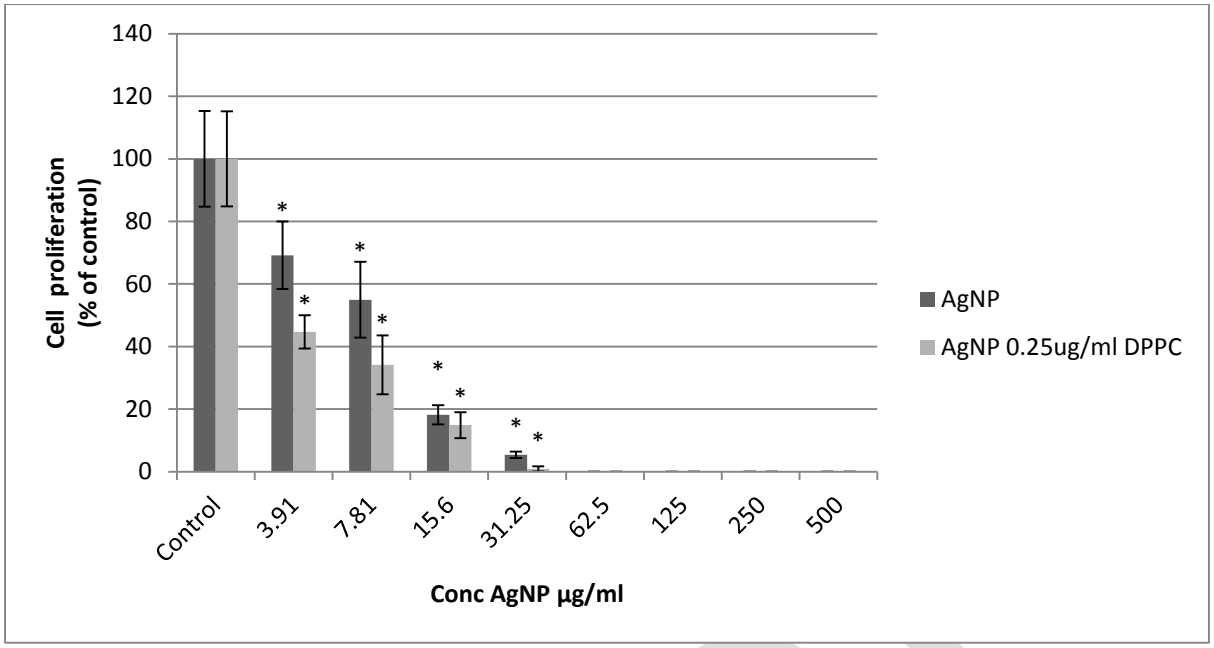

Figure 5 Cytotoxicity of AgNP alone and with added DPPC after 10 day exposure as determined by the clonogenic assay. Data are expressed as percentage of control mean ± SD of four independent experiments. * denotes a statistically significant ($p<0.05$) difference from the unexposed control

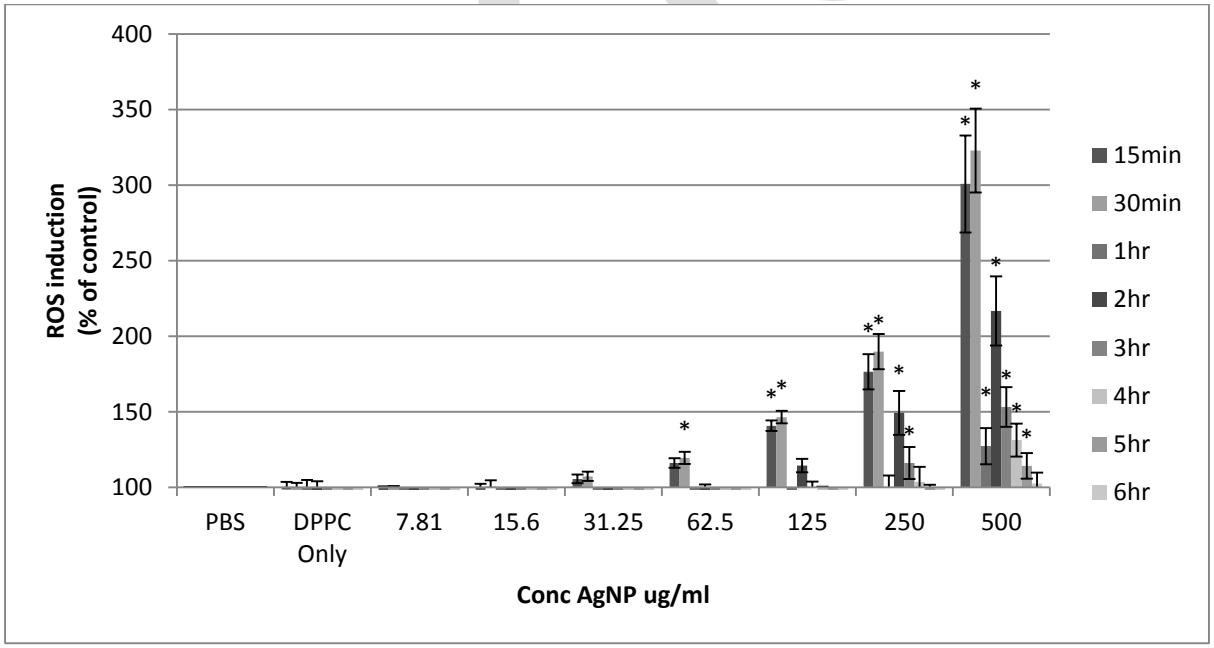

Figure 6 ROS generation in A549 cells after different time points of AgNP exposure in the presence of DPPC. Data expressed as percentage of control mean ± SD of eight independent experiments. * denotes a statistically significant ($p<0.05$) difference from the unexposed control

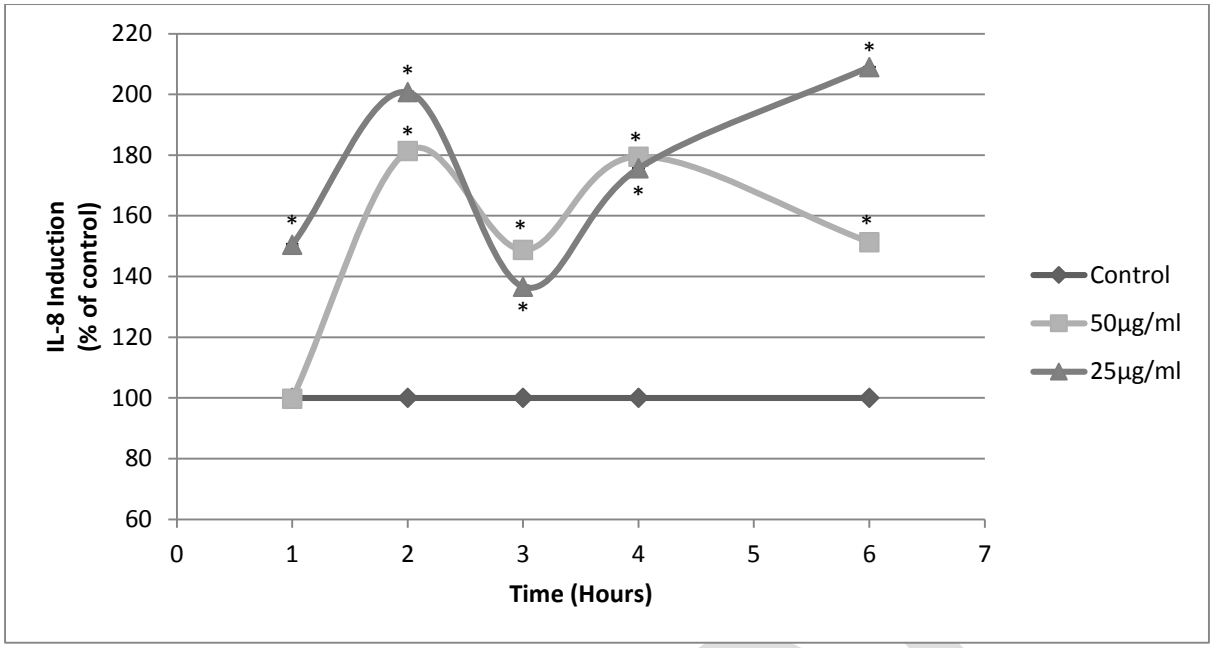

Figure 7 Induction of IL-8 in A549 cells at 1-4 and 6 hours following exposure to AgNP. Data expressed as percentage of control mean ±SD of three individual experiments. * denotes a statistically significant ($p<0.05$) difference from the unexposed control

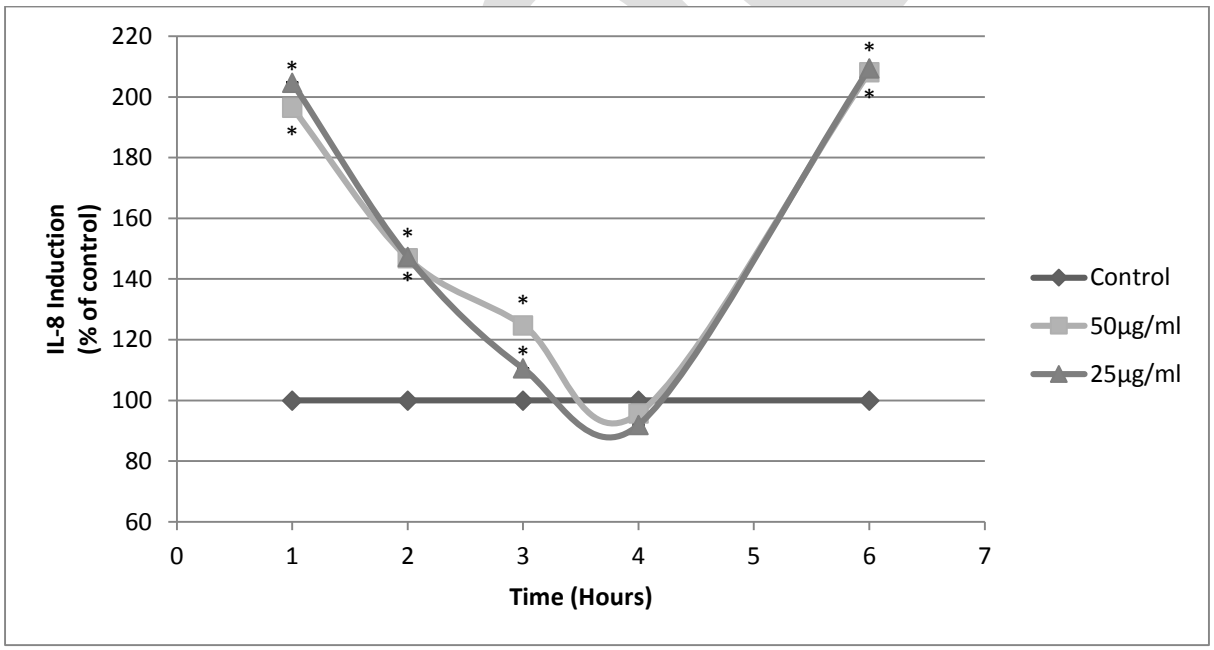

Figure 8 Induction of IL-8 in A549 cells at 1-4 and 6 hours following exposure to AgNP in the presence of DPPC. Data expressed as percentage of control mean ±SD of three individual experiments. * denotes a statistically significant ($p<0.05$) difference from the unexposed control

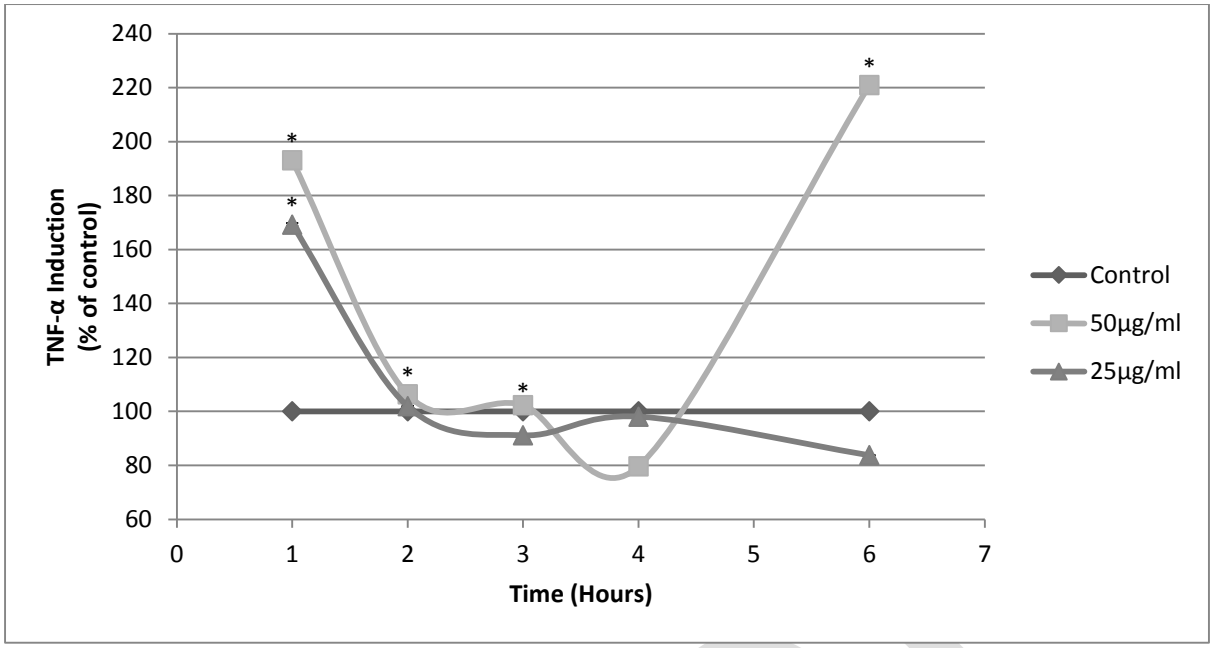

Figure 9 Induction of TNF-α in A549 cells at 1-4 and 6 hours following exposure to AgNP. Data expressed as percentage of control mean ±SD of three individual experiments. * denotes a statistically significant ($p<0.05$) difference from the unexposed control

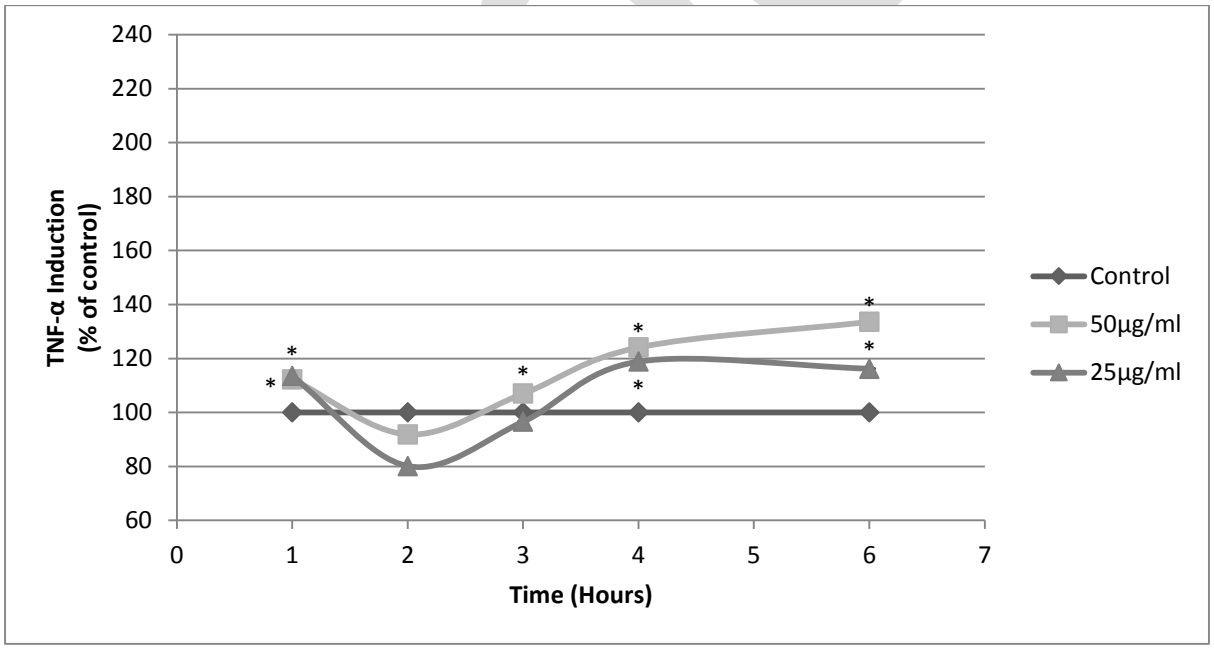

Figure 10 Induction of TNF-α in A549 cells at 1-4 and 6 hours following exposure to AgNP in the presence of DPPC. Data expressed as percentage of control mean ±SD of three individual experiments. * denotes a statistically significant ($p<0.05$) difference from the unexposed control